

Discovery and Optimization of WDR5 Inhibitors via Cascade Deoxyribonucleic Acid-Encoded Library Selection Approach

Shaozhao Qin,[#] Lijian Feng,[#] Qingyi Zhao, Ziqin Yan, Xilin Lyu, Kaige Li, Baiyang Mu, Yujie Chen, Weiwei Lu, Chao Wang, Yanrui Suo, Jinfeng Yue, Mengqing Cui, Yingjie Li, Yujun Zhao,* Zhiqiang Duan,* Jidong Zhu,* and Xiaojie Lu*Cite This: *J. Med. Chem.* 2024, 67, 1079–1092

Read Online

ACCESS |



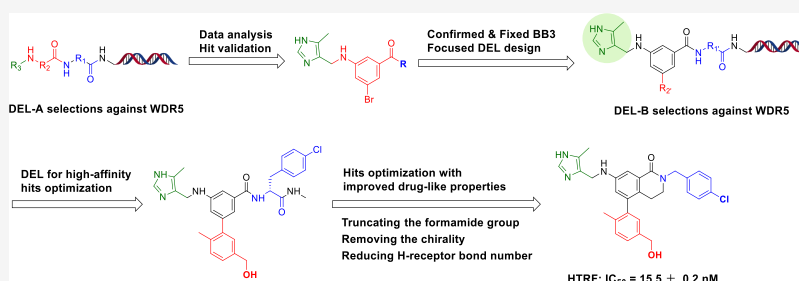
Metrics & More



Article Recommendations



Supporting Information



ABSTRACT: The DNA-encoded library (DEL) is a powerful hit generation tool for chemical biology and drug discovery; however, the optimization of DEL hits remained a daunting challenge for the medicinal chemistry community. In this study, hit compounds targeting the WIN binding domain of WDR5 were discovered by the initial three-cycle linear DEL selection, and their potency was further enhanced by a cascade DEL selection from the focused DEL designed based on the original first run DEL hits. As expected, these new compounds from the second run of focused DEL were more potent WDR5 inhibitors in the protein binding assay confirmed by the off-DNA synthesis. Interestingly, selected inhibitors exhibited good antiproliferative activity in two human acute leukemia cell lines. Taken together, this new cascade DEL selection strategy may have tremendous potential for finding high-affinity leads against WDR5 and provide opportunities to explore and optimize inhibitors for other targets.

INTRODUCTION

WDR5, belonging to the WD40 protein family, acts as an essential central scaffold in various protein complexes that relate to epigenetic mechanisms and transcriptional regulation.¹ WDR5 contains two major binding interfaces, the WDR5 binding motif (WBM) and WDR5 interaction motif (WIN) sites, which accommodate diverse partner proteins.² Mixed-lineage leukemia 1 (MLL1) is one of the well-characterized protein–protein interaction partners that bind on the WIN site of the WDR5 using a conserved arginine as an anchor.³ MLL1-WDR5 interaction is crucial to maintain the integrity and catalytic activity of the MLL1 complex.⁴ More importantly, recent studies suggested that the MLL complex is essential to maintaining an oncogenic gene expression program in human leukemias harboring MLL rearrangement (MLL-r), and knock-down of WDR5 results in significantly suppressed growth of MLL-r leukemias.⁵ These results indicate that blocking the WDR5-MLL1 interaction may be an effective strategy for treating acute leukemia.⁶ To date, a remarkable number of WDR5 WIN-site inhibitors have been discovered, and typical examples are listed in Figure 1. For instance, Wang and colleagues reported several peptide inhibitors of WDR5 WIN domain, including the cyclic peptide MM-589, which

stands out as arguably the most potent peptide inhibitor to date.⁷ WDR5-0102 is the first nonpeptidic inhibitor of the WIN site discovered from the fluorescence polarization-based high-throughput screening.⁸ WDR5-MLL1 inhibitor DDO-2213 contains a new aniline pyrimidine scaffold and was produced utilizing a scaffold-hopping strategy from a benzamide inhibitor.⁹ Fesik and co-workers described a series of inhibitors via fragment-based screening and structure-based optimization (6e; WDR5-IN-1; WDR5-IN-5).^{10–12} In addition, several proteolysis-targeting chimera molecules were obtained by linking known WIN site inhibitors to E3 ubiquitin ligases using a suitable linker.¹³ Nowadays, the exploration of drugs that specifically target WDR5 as a therapeutic strategy is still in its infancy, and no WDR5-targeting drug has been approved for clinical use. Therefore, more new inhibitors with structural diversity targeting WDR5 are in urgent need.²

Received: August 9, 2023

Revised: November 29, 2023

Accepted: December 13, 2023

Published: January 3, 2024



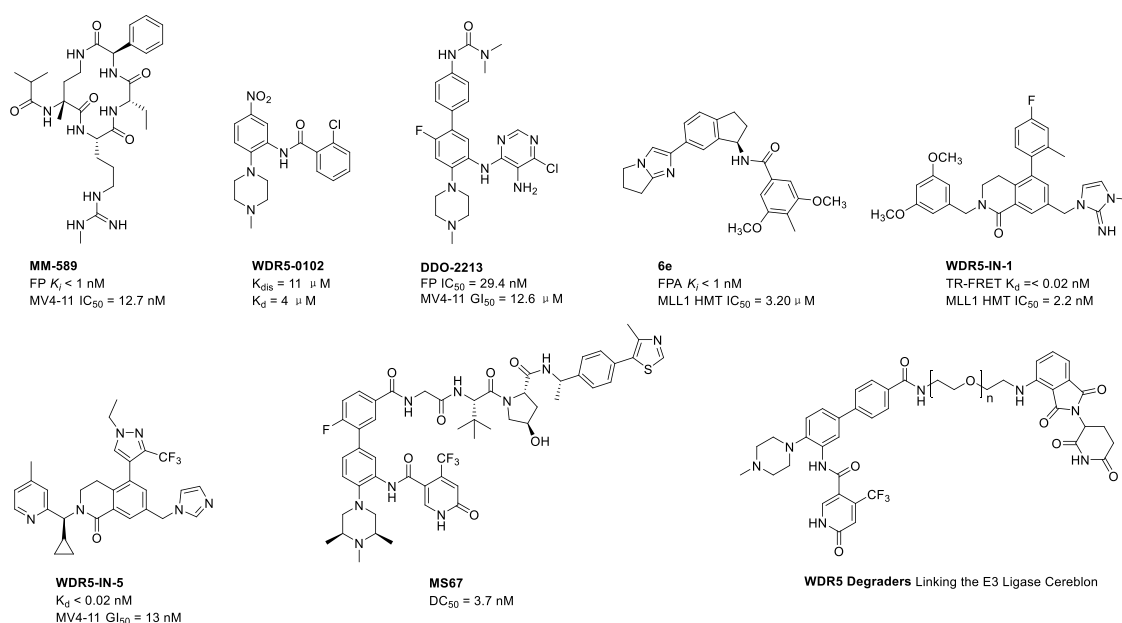


Figure 1. Representative inhibitors and degraders targeting the WDR5 WIN domain.

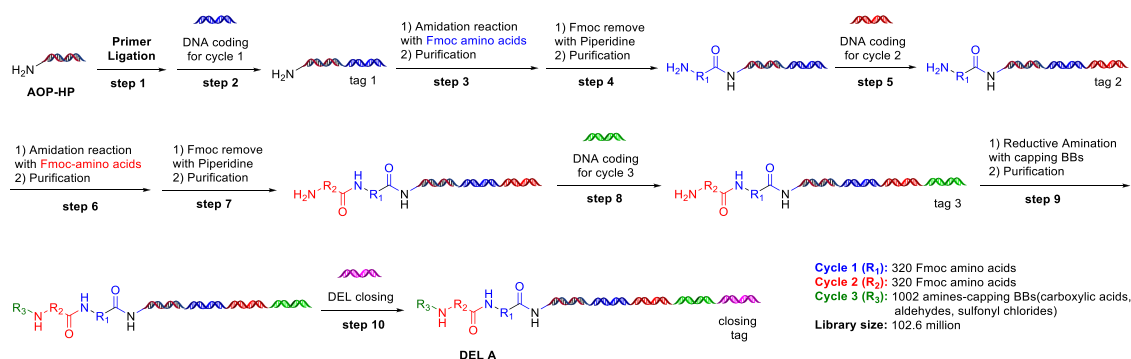


Figure 2. Synthetic schemes for DEL-A.

Recent years have witnessed increasing attention concentrated on the DNA-encoded library (DEL) technology maturing as a cutting-edge approach for chemical biology and drug discovery.^{14–16} Since originally proposed by Brenner and Lerner,¹⁷ various DELs with substantial compounds in chemical structures and chemical space have been well-established for pharmaceutical hit discovery.^{18,19} Among them, focused DELs with structural and functional features are attracting substantial interest due to its potential for effectively generating libraries and discovering novel hits within a specific protein class.^{20,21} For example, Franzini et al. reported a focused DEL to target NAD^+ binding pockets and explored the chemical binder space of enzymes with ADP-ribosyltransferase activity.²² Krusemark et al. designed a protease-focused DEL that contains guanidine moiety to engage with the conserved catalytic protease residues and revealed several potent thrombin binders after selection.²³ Disney et al. applied an RNA-focused DEL to identify an $r(CUG)^{exp}$ binder that improves DM1-associated defects.²⁴ Furthermore, focused DELs can offer robust capabilities for extensive exploration of structure–activity relationships (SAR), enabling medicinal chemists to design specialized DELs, such as covalent modifiers, macrocycles, and intricate natural products.^{25–27}

The optimization of hits is a crucial phase in the exploration and development of novel chemical compounds through DELs. Several effective methods for optimizing DEL hits have been employed, such as virtual screening, SAR analysis, and guidance from cocrystal structures.^{28,29} More importantly, selections using library retooling is considered another valuable strategy to enhance the discovery of active ligands due to the DEL inherent advantages.^{30–33} For example, using two generations of directed DELs, Dykhuizen et al. reported hit identification and subsequently further optimization to increase potency, cell permeability, and selectivity.³⁴

Inspired by these previous pioneering works, in the present work, we described a new DEL selection strategy utilizing a cascade DEL selection to discover and enhance the hit potency of a novel series of WDR5 inhibitors targeting the WIN site. We initially attempted to identify binders against WDR5 using our three-cycle linear DEL (termed DEL-A) through affinity selection experiments. After PCR amplification, deep sequencing, and off-DNA compounds testing in the homogeneous time-resolved fluorescence (HTRF) assay, we obtained some novel binders against the WIN site of WDR5. More importantly, preferentially enriched new building block (BB) 5-methyl-1H-imidazole was identified and confirmed as having a crucial role in binding to the arginine binding pocket of WDR5 WIN. Subsequently, we designed and synthesized a

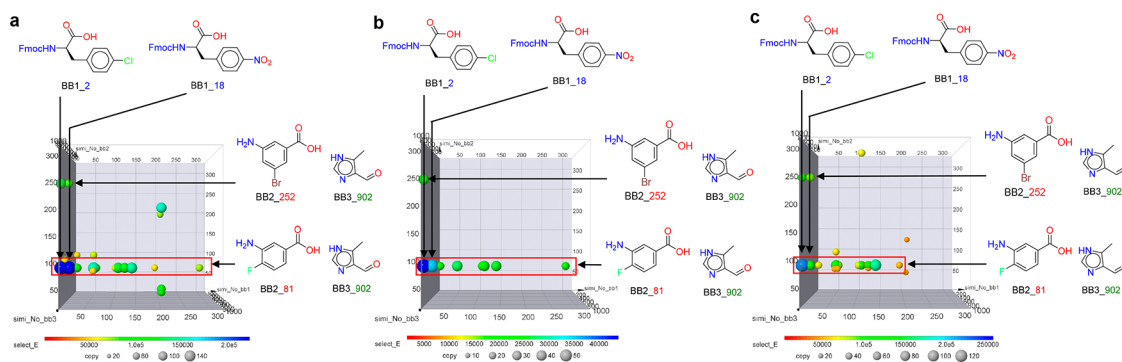


Figure 3. Selection of DEL-A against WDR5. (a) Selection output from DEL-A selections against WDR5 (His tag). Count cutoff filter (<40 copies). Both selections show lines in cycle 3 corresponding to 5-methyl-1*H*-imidazole. (b) Selection output from DEL-A selections against WDR5 (biotin tag). Count cutoff filter (<20 copies). (c) Selection output from DEL-A selections against WDR5 (His tag) competed away by a known WBM site antagonist (peptide AHx-SEEEIDVVSV). Count cutoff filter (<20 copies).

Table 1. In Vitro Inhibitory Activity of Compounds against WDR5/MLL1 Interaction

Compd.	R ₁	R ₂	IC ₅₀ ± SD (nM) ^a	Compd.	R ₁	R ₂	IC ₅₀ ± SD (nM) ^a
1		2-F	84.6 ± 3.1	4		4-Br	220.7 ± 30.6
2		2-F	239.2 ± 22.6	5		4-Br	25.2 ± 5.9
3		4-Br	50.0 ± 2.9	6		4-Br	32.4 ± 7.1
WDR5-IN-1		positive control	6.8 ± 0.2				

^aMean value of at least twice enzyme activity assays.

focused DEL (termed DEL-B) featuring fixed 5-methyl-1*H*-imidazole as a capping reagent to further develop more potent binders. As expected, a few new potency binders derived from DEL-B were verified after affinity selection and off-DNA compound testing. Furthermore, we selected the representative inhibitors and evaluated their cellular functions in two human acute leukemia cell lines.

RESULTS AND DISCUSSION

DEL Affinity Selection and Hit ID. We initially tried to perform affinity selection experiments employing DEL-A to identify binders against WDR5. The construction of this three-cycle linear DEL involved employing a split-and-pool combinatorial chemical strategy and incorporating a wide range of amino acids and capping reagents to create compounds with three distinct chemical BBs. As shown in Figure 2, its synthesis started by conjugation of DNA headpiece (a short sequence of duplex DNA, HP) appended with Fmoc-15-amino-4,7,10,13-tetraoxapentadecanoic acid (AOP), which served as a spacer to keep a distance from DNA and small-molecule. After the enzymatic priming step (step 1) on the AOP-HP, the resulting products were divided into 320 wells, each of which was then labeled with a distinct barcoding DNA (tag1) corresponding to the first set of chemical BBs (step 2). Subsequently, BB conjugation was

executed through an amidation reaction with the corresponding 320 amino acids within each well, giving the first cycle of the library product (cycle 1, step 3). After pooling, deprotection of the N-Fmoc, and purification, DNA-conjugated intermediates were again split into 320 wells to install the cycle 2 DNA tags and cycle 2 BBs, resulting in the desired DNA material (steps 5 and 6). These resulting products were also subjected to pooling, N-Fmoc deprotection, and purification (step 7) before being further split into 1002 wells for the final transformation step. Cycle 3 was achieved by installing a set of acids, aldehydes, and sulfonyl chlorides as capping reagents after ligation to a third DNA barcode (steps 8 and 9). The conjugates were then pooled and ligated with the closing tag (step 10), generating the final library comprising 102.6 million different three-cycle compounds. Subsequently, we performed a series of affinity selections under various conditions using DEL-A that was incubated with WDR5, which was first immobilized onto magnetic beads through tags (either His tag or biotin tag) (Figure 3). Figure 3a shows the DEL-A selection performed using the His-tagged WDR5. Simultaneously, a tag control group selection was conducted using biotin-tagged WDR5 to determine whether the enrichment signal resulted from tag binding (Figure 3b). Additionally, Figure 3c details the DEL selection performed with the His-tagged WDR5 in the presence of positive inhibitors

targeting the WBM site. In addition, we performed DEL selection without the target protein (no target control, NTC) to recognize nonspecific binders to the bare beads as a control. In Figure 3, each sphere presented an encoded compound in a three-dimensional space, in which the x -, y -, and z -axes represent individual BBs at the indication of each cycle. The sphere color corresponds to the DNA sequence counts, while the sphere size is proportional to the select_E value of the corresponding DNA tag. Furthermore, we proposed a count cutoff to filter out most compounds with low read counts and only display selection results that had reached a minimal level of sequence counts. As shown in Figure 3a, some distinct selections were defined by preferentially enriched BB3 (BB3_902, 5-methyl-1H-imidazole) with some specific BB1 (BB1_2, BB1_18) and BB2 (BB2_81, BB2_252) combination. This illustrates the significant role of BB3_902 together with certain BB1 and BB2 elements in their binding to WDR5. These special BBs were also observed to have enriched in tag control group selection, indicating the enrichment binders do not stem from tags (Figure 3b). Notably, the signals were also present in the WBM competition group, meaning the binding site presumably was the WIN pocket but not the WBM site (Figure 3c). Furthermore, there was no obvious feature in the NTC group (Supporting Information for details, Figure S4).

Hit Confirmation. We next synthesized some representative off-DNA compounds 1–3 from the structure of the enriched features with the highest counts to determine whether the building block combinations could inhibit the activity of WDR5. These compounds were evaluated in an HTRF assay to determine the inhibition of WDR5 and MLL peptide complexes with IC₅₀ values of 84.6, 239.2, and 50.0 nM (Table 1). Among the validated compounds, 1 and 3 with a 4-chlorobenzyl group at the BB1 exhibited high inhibitory ability. Compound 3 containing 4-bromo substitution at BB2 exhibited nearly 2-fold increased biological activities than 1. Additionally, further changing R₁ from 4-chlorobenzyl to 4-nitrophenyl gave compound 2, resulting in a significant reduction in the inhibitory activity, implying that nitrophenyl is not beneficial.

Based on these results, we performed a limited SAR study by synthesis of compounds 4–6, whose BB3 was fixed to the 5-methyl-1H-imidazole (Table 1, 4–6). The inhibitory ability of 4 was more than 4-fold less potent than 3, suggesting that the carboxyl on BB1 was beneficial for increased inhibitory activity. Moreover, when carboxyl was replaced with a methyl amide to produce compound 5, it demonstrated a 2-fold increase in potency. This indicates that the transformation from a carboxylic acid to a methyl amide is beneficial for enhancing potency. Additionally, compound 6 with cyclopropyl amide gave slightly reduced potency compared to 5.

In order to confirm the binding mode with the WDR5 protein, we conducted a molecular docking of 5 into the WIN site. Docking results indicated that 5-methyl-1H-imidazole moiety binds deep into the arginine binding pocket (S2) subsite to form strong sandwiched π – π stacking interactions with F112 and F242. In addition, the nitrogen atom at the 3-position of the imidazole formed a hydrogen bond with the backbone carbonyl of Ser 70. The binding module indicated that 5-methyl-1H-imidazole can insert into the arginine binding pocket at the central cavity and is crucial to maintain the affinity with the WIN site (Figure 4). The amino group of the BB2 formed a direct hydrogen bond with the side chain of Cys240, and a similar interaction was formed between the

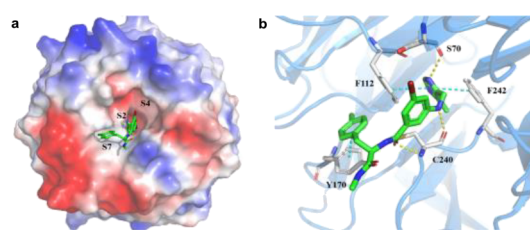


Figure 4. Docking studies on WDR5 and 5. (a) Compound 5 (green-carbon capped sticks) bound to WDR5 is represented as a semitransparent electrostatic potential surface with S2 and S7 binding regions denoted. (b) Key H-bond (yellow dashed lines) and π – π stacking interaction residues of WDR5 that interact with 5.

carbonyl group of the BB2 with the Cys240. Furthermore, the phenyl ring of BB1 also π -stacks similarly to the Tyr170. More importantly, the binding mode from the docking study demonstrated no group of 5 occupying the S4 pocket, which could guide the design of more potent WIN inhibitors.

Focused DEL Construction and Hit ID. To further explore more potent binders that inhibit WDR5 via the WIN site, we pursued a focused DEL (DEL-B) approach to identify novel and powerful hits for binding to WDR5. DEL-B was also constructed employing a split-and-pool synthesis procedure. This focused DEL featured anchoring 5-methyl-1H-imidazole into the design of this library for binding to the arginine binding pocket (S2). Meanwhile, 357 boron reagents with varying substitution patterns and sizes were taken to react with 4-bromo at BB2 to occupy the S4 pocket. As described in Figure 5, AOP-HP is linked to 124 amino acids through amide bond formation in cycle 1. The resulting DNA conjugates were then coupled to 3-amino-5-bromobenzoic acid, which was taken as a core scaffold with bromine substitution in the ortho position. Following further reaction with a fixed capping reagent 5-methyl-1H-imidazole by reductive amination, the DNA-coupled intermediate subsequently underwent the Suzuki–Miyaura coupling with 357 boron reagents to afford the focused DEL comprising 44268 different two-cycle compounds. Next, we conducted an affinity selection experiment using the so-yield DEL-B incubated with WDR5 protein, taking an NTC selection as the control (Figure 6). As displayed in Figure 6a, the most strongly enriched structure in cycle 1 was also the 4-chlorobenzyl group with some preferentially coenriched BB2 was identified. Additionally, it was found that (2-(methylthio) phenyl) boronic acid (BB_96) was preferred at cycle 2. A representative set of the selected molecules without the DNA tag was chosen based on copy number and synthesized according to the route illustrated in Scheme 2. The prepared compounds were then assayed for their biochemical activity against WDR5 and MLL peptide complexes (Table 2). Compound 7 displayed nearly 3-fold enhanced inhibition than 3, suggesting that occupying the S4 pocket was beneficial for potency. Compound 8 containing 2-cyclopropyl group at R₁ also exhibited high potency ability. Both 5-(hydroxymethyl)-2-methyl and 4-chloro-2-trifluoromethyl derivatives (9 and 10) still had strong inhibitory IC₅₀ values (8.8 \pm 0.4 nM and 19.8 \pm 0.1 nM, respectively). In addition, 11 showed a significant decrease in inhibition, suggesting that substitution at the ortho position is unfavorable (IC₅₀ = 148.7 \pm 28.1 nM). Taking all these results together, the data indicate that the cascade DEL selection approach is promising in the exploration and optimization of potent inhibitors against WDR5.

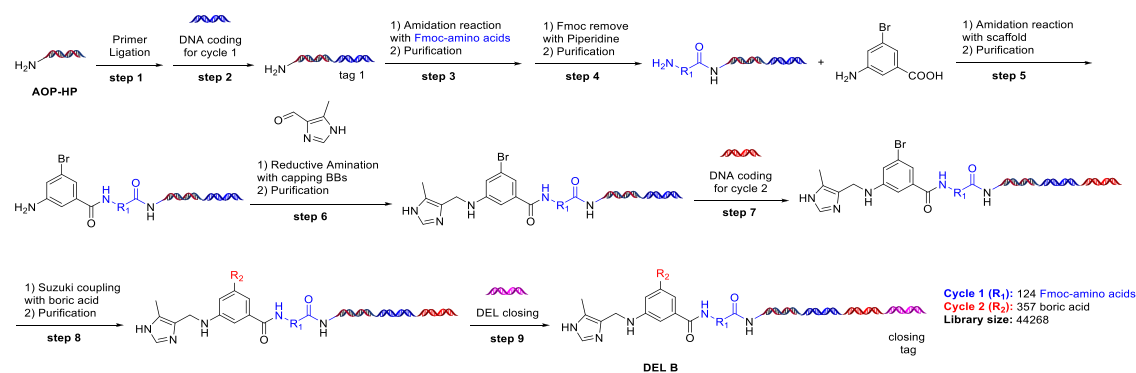


Figure 5. Synthetic schemes for DEL-B.

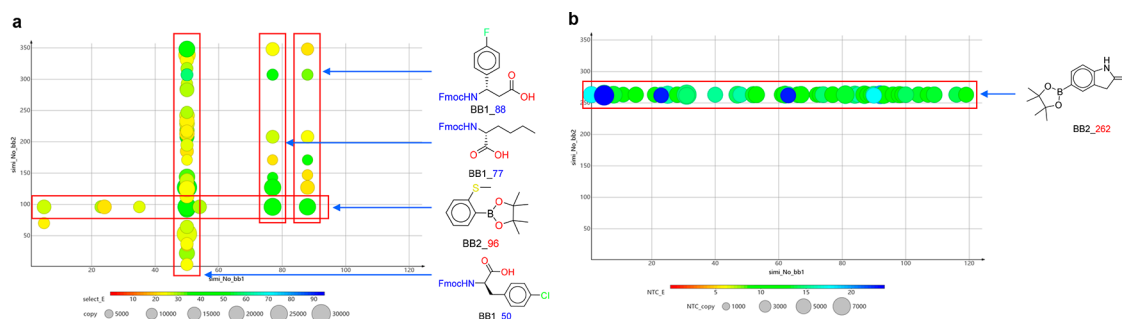


Figure 6. Selection of DEL-B against WDR5. (a) Selection output from DEL-B selections against WDR5. Count cutoff filter (<10000 copies). (b) NTC selection output from DEL-B. Count cutoff filter (<2000 copies).

Table 2. In Vitro Inhibitory Activity of Compounds 7–11 against WDR5/MLL1 Interaction

Compd.	R ₁	IC ₅₀ ± SD (nM) ^a	Compd.	R ₁	IC ₅₀ ± SD (nM) ^a
7		11.3 ± 1.9	10		19.8 ± 0.1
8		18.8 ± 1.7	11		148.7 ± 28.1
9		8.8 ± 0.4	WDR5-IN-1	positive control	6.4 ± 0.2

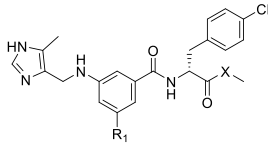
^aMean value of at least twice enzyme activity assays.

Cell-Based Assessment. Based on their good activity in HRTF binding assay, 7, 9, 12, and 13 were selected and their antiproliferative activity were evaluated against two human acute leukemia cell lines, MV4–11 harboring MLL-r and K562 without the MLL-r (Table 3). WDR5-IN-1 (Figure 1) was also included as a positive control, while all compounds inhibited the cell growth of MV4–11 and K562 with IC₅₀ values in the low micromolar range. In more detail, 7 has cell growth inhibitory IC₅₀ values of 1.9 μM and 1.1 μM in MV4–11 and K562 cell lines, respectively. Replacement of the methyl amide group of 7 by a methyl ester on BB1 gave compound 12, resulting a slight increase in antiproliferative activity (IC₅₀ =

3.9 μM and 3.0 μM, respectively). However, the inhibitory IC₅₀ values of 9 and 13 increased significantly (IC₅₀ = 5.0 μM and 12.2 μM; 5.5 μM and 4.9 μM, respectively). Notwithstanding, the current cellular results indicated that this new cascade DEL selection approach is not compatible with cellular activity optimization.

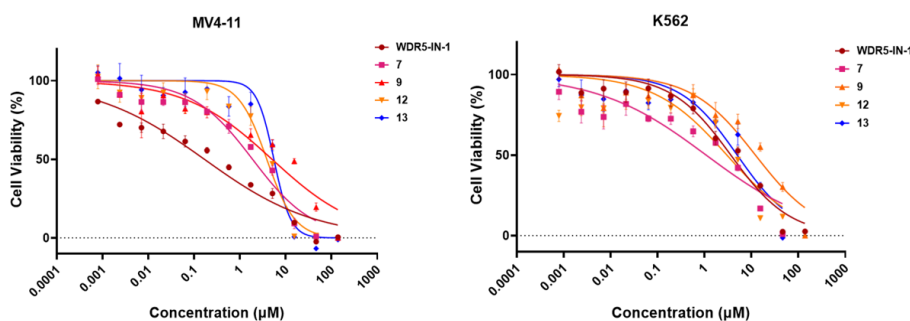
To improve drug-like properties and enhance antiproliferative efficacy, we conducted a redesign and synthesized new compounds 14–21 with improved drug-like properties (Table 4). Optimization strategies included truncating the formamide group and removing the chirality on BB1, reducing molecular weight, H-receptor, and acceptor bond numbers, and employ-

Table 3. Cell Growth Inhibition Evaluation and Curves of Representative Compounds in MV4-11 and K562 Human Leukemia Cell Lines



Compd.	R ₁	X	IC ₅₀ (μM) ^a		Compd.	R ₁	X	IC ₅₀ (μM) ^a	
			MV4-11	K562				MV4-11	K562
7		NH	1.9 ± 0.2	1.1 ± 0.3	9		NH	5.0 ± 0.3	12.2 ± 1.7
12		O	3.9 ± 0.1	3.0 ± 0.1	13		O	5.5 ± 0.4	4.9 ± 0.3
WDR5-IN-1	positive control		0.17 ± 0.02	3.6 ± 0.5					

^aThe IC₅₀ values were mean of at least two independent experiments.



^aThe IC₅₀ values were mean of at least two independent experiments.

ing a tether design strategy to establish the dihydroisoquinoline as a fixed conformational scaffold. Most of these obtained compounds gave protein inhibitory IC₅₀ values between 10 and 100 nM, with **20** exhibiting the highest inhibitory IC₅₀ value of 15.5 ± 0.2 nM. The results suggest that these compounds are of relatively good activity toward the inhibition of WDR5 and MLL peptide complexes. Meanwhile, these compounds exhibited mild antiproliferative activities in two human acute leukemia cell lines. Compound **21** demonstrated the most promising cellular inhibitory activity within this series. While these optimizations did not yield compounds with significantly enhanced cellular inhibitory activity, these compounds showed promising characteristics as potential compounds with improved drug-like properties. Our ongoing efforts aim to further optimize these compounds based on these promising results, intending to enhance antiproliferative activity and refine their drug-like attributes.

Chemistry Synthesis. Scheme 1A illustrates the general synthetic pathway for the representative compounds 1–3. The synthesis began with the amine ester, which underwent amide coupling with acids to form **23a–c**. These intermediates then underwent reductive amination with compound **24**, resulting in the respective products. Finally, the desired compounds were obtained after ester hydrolysis. Compounds **4–6** were synthesized following a similar reaction sequence as described in Scheme 1B,C. Compounds **7–11** followed a comparable synthesis route, commencing from the amine ester and ultimately yielding the desired products via the Suzuki–

Miyaura cross-coupling reaction with corresponding boronic acids (Scheme 2).

Scheme 3A illustrates the synthesis of compounds **14** and **16–21**. It began with the hydrolysis of commercially available compound **28** under concentrated HCl, resulting in the creation of intermediate **29**. This intermediate underwent reductive amination with compounds **30a–b**, giving compounds **31a–b**. In the presence of Ti(OC₃H₇)₄, the cyclization reaction of **31a–b** facilitated the construction of the dihydroisoquinoline scaffold, thereby producing **32a–b**. Reduction of the nitro group within **32a–b** yielded compounds **33a–b**, which were subsequently transformed through reductive amination into compounds **34a–b**. These compounds then underwent Suzuki–Miyaura cross-coupling reactions with corresponding boronic acids, ultimately yielding compounds **14** and **16–21**. The preparation of compound **15** was initiated from compound **35**, which underwent a substitution reaction with 1-(2-bromoethyl)-4-chlorobenzene, resulting in the generation of intermediate **37**. Then, following a similar reaction sequence as described in Scheme 3A, the target compound **15** was generated (Scheme 3B).

CONCLUSIONS

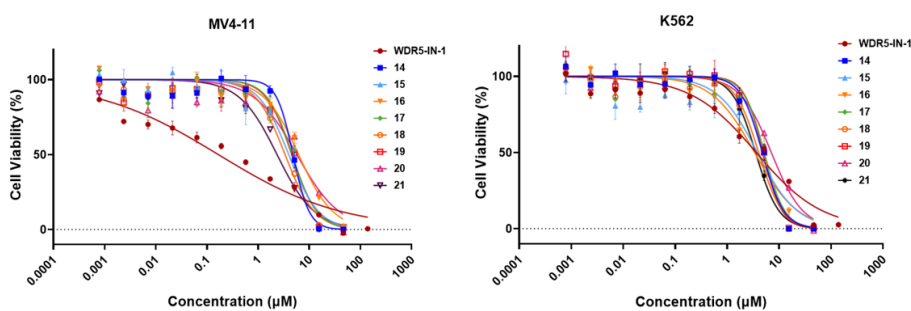
In conclusion, we designed a new cascade DEL selection approach to discover and enhance the potency of hits about a novel series of WDR5 inhibitors targeting the WIN site. We initially constructed a three-cycle linear DEL composed of 102.6 million encoded small molecules. Then, some novel binders were verified after affinity selection and off-DNA

Table 4. In Vitro Inhibitory Activities of Compounds 14–21 against the WDR5/MLL1 Interaction and Their Cell Growth Inhibition Activities in MV4-11 and K562 Human Leukemia Cell Lines With the Inhibitory Curves Attached At the End

Compd.	n	R ₁	R ₂	IC ₅₀ ± SD (nM) ^a	IC ₅₀ (μM) ^b	
					MV4-11	K562
14	1			41.6 ± 4.3	4.8 ± 0.6	4.7 ± 0.7
15	2			319 ± 59.7	3.9 ± 0.4	3.8 ± 0.8
16	1			17.2 ± 1.3	6.2 ± 0.4	3.4 ± 1.5
17	1			75.8 ± 9.7	4.6 ± 0.1	5.2 ± 0.6
18	1			39.5 ± 0.6	3.5 ± 0.8	4.0 ± 0.9
19	1			40.5 ± 6.8	4.6 ± 0.6	4.9 ± 0.1
20	1			15.5 ± 0.2	5.7 ± 0.6	7.1 ± 1.9
21	1			26.9 ± 5.5	2.3 ± 0.5	3.5 ± 0.2
WDR5-IN-1		Positive control			0.17 ± 0.02	3.6 ± 0.5

^aMean value of at least twice enzyme activity assays.

^bThe IC₅₀ values were mean of at least two independent experiments.

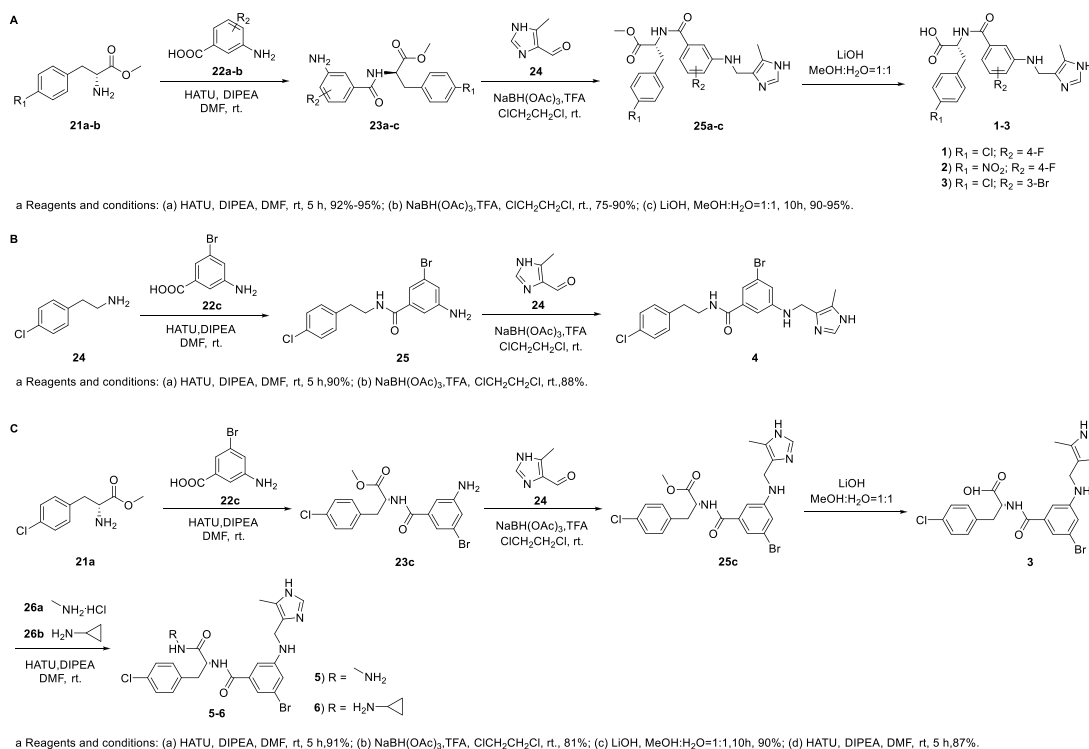


^aMean value of at least twice enzyme activity assays. ^bThe IC₅₀ values were the mean of at least two independent experiments.

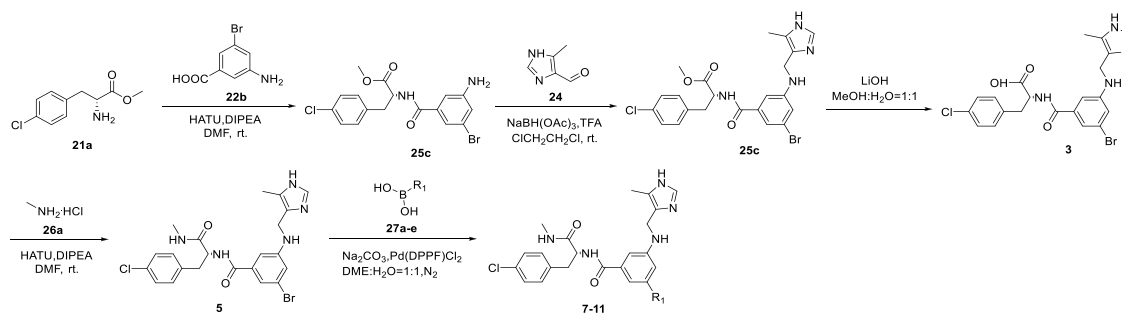
compound testing in HTRF. Following further SAR studies led to the discovery of compound **5** with an inhibitory IC₅₀ value of 25.2 ± 5.9 nM. More importantly, a preferentially enriched new BB 5-methyl-1H-imidazole was identified from the three-cycle linear DEL and confirmed to have a crucial role in binding to the WIN arginine binding pocket based on docking studies. Subsequently, we designed and constructed a focused DEL featuring fixed 5-methyl-1H-imidazole as a capping reagent for binding to the arginine binding pocket (S2) and coupling to the multiplicity structures of boron reagents for occupying the WIN S4 pocket to explore more potent binders.

As expected, we obtained several strong inhibitory binders derived from DEL-B, and **9** gave the most efficient WDR5 inhibitory activity (8.8 ± 0.4 nM). In addition, we selected the representative inhibitors and evaluated their antiproliferative activity against two human acute leukemia cell lines (MV4–11 and K562) and all compounds showed micromolar level inhibitory potencies. In addition, we conducted a redesign and synthesized new compounds **14–21** with improved drug-like properties. Ongoing efforts are focusing on further enhancing the antiproliferative activity and refining their drug-like attributes. More importantly, this new cascade DEL selection

Scheme 1. Synthesis of Representative Compounds from DEL-A Off-DNA



Scheme 2. Synthesis of Representative Compounds from DEL-B Off-DNA



approach may represent a significant strategy to generate high-affinity hits and play a role in exploring and optimizing inhibitors against WDR5 and other targets.

EXPERIMENTAL SECTION

General Methods. All commercial reagents and anhydrous solvents were utilized directly unless specified otherwise. The progression of reactions was monitored through liquid chromatography–mass spectrometry (LC-MS) on an Agilent 6125B equipped with an SB-C18 reversed-phase column (250 mm × 4.60 mm, 5 μm) or thin-layer chromatography (TLC). ¹H and ¹³C NMR spectra were obtained using a Bruker Advance NMR 500 spectrometer, and chemical shifts are reported in parts per million (ppm), referencing TMS as the internal standard. For ¹H NMR data, abbreviations include coupling constants (Hz) and multiplicity (singlet, s; doublet, d; triplet, t; quartet, q; heptet, h; multiplet, m; and broad signal, bs). High-resolution mass spectrometry (HRMS) analysis was conducted using UHPLC-QTOF (Agilent Corporation) and Thermo DFS (Thermo Fisher Scientific). LC-MS analysis was performed on an Agilent 6125B with SB-C18 reversed-phase column (250 mm × 4.60 mm, 5 μm). Purification of the final product employed a SunFire Prep C18 OBR 5 μm, 19 mm × 150 mm column with a 10 mL/min flow rate. Solvent A comprised 0.1% TFA in water, while Solvent B was CH₃CN. The purity of the final compounds was assessed using a

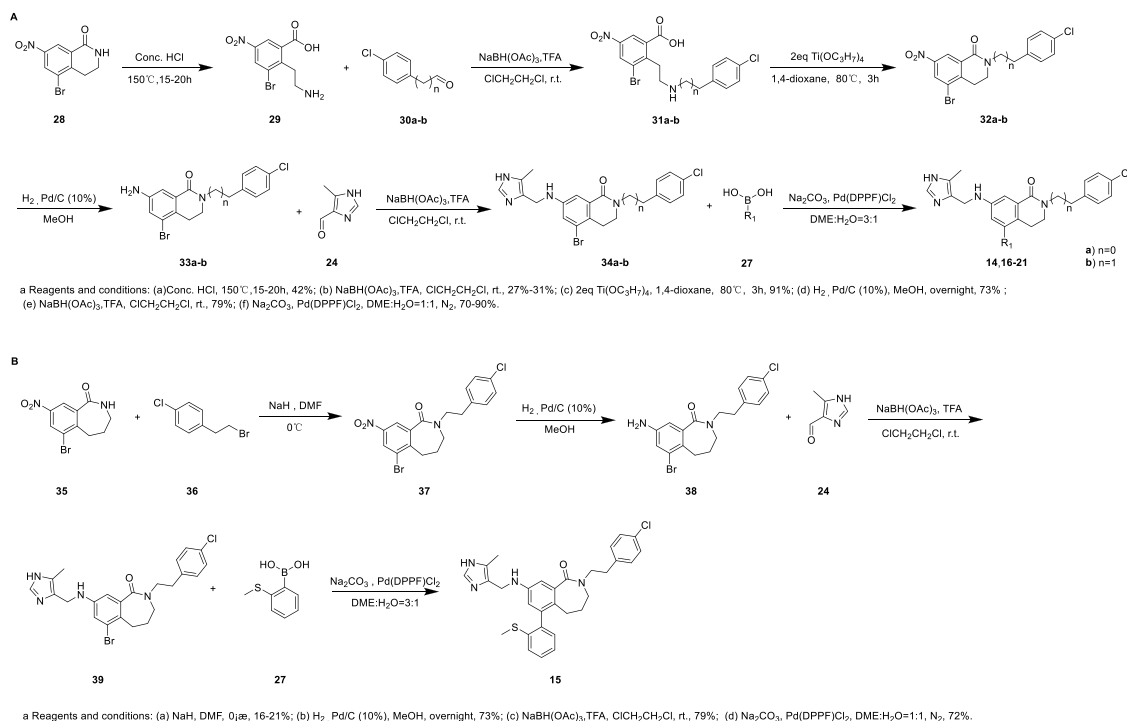
SHIMADZU LC20-AR with a SunFire C18 column (5 μm, 4.6 mm × 150 mm) or the Waters UPLC H class with an ACQUITY UPLC BEH C18 column (1.7 μm, 2.1 mm × 50 mm). The purity of all biologically tested compounds exceeded 95%.

General Procedure for DNA Ligation. The DNA-conjugated compounds were initially diluted with ddH₂O (1.1 eq, V/V) in a 1.5 mL centrifuge bottle. Subsequently, 1.1 eq of a 1.8 mM DNA tag, 10% of the volume of a 10× T4 ligation buffer, and 30 eq of T4 ligase (600,000 U) were added in sequence. Following this, the ligation system was further diluted to 0.25 mM with ddH₂O. The mixture was vortexed and left at room temperature for 16 h. After confirming the completion of ligation by HPLC/ESI-MS, the DNA-linked product was isolated through ethanol precipitation.

Ethanol Precipitation for DNA Recovery. Into the DNA reaction mixture, a 10% (v/v) solution of 5 M NaCl and 2.5 times the volume of cold absolute ethanol (stored at –80 °C) were added. After thorough mixing, the resulting solution was allowed to incubate at –80 °C for 30 min. Subsequently, the solution was centrifuged at 4 °C in a microcentrifuge (10,000 × g for 30 min at 10 K rpm). Following the removal of the supernatant, the pellet (precipitate) was rapidly cooled in liquid nitrogen and then desiccated through vacuum drying using a lyophilizer to obtain the dry pellet.

General Procedure for Quantification DNA. Initially, the DNA intermediate was subjected to centrifugation in a microcentrifuge

Scheme 3. Synthesis of Compounds 14–21



within a spin-filter tube (3 K) at 4 °C (30 min, 10 K rpm), repeated three times. Subsequently, the purified DNA compound was quantified using a Thermo Scientific™ NanoDrop™ One in ds-DNA mode.

DEL Screening. Biotin or His-tagged WDR5 (5.0 μg) in 100 μL of selection buffer [Biotin:1× PBS (pH 7.4), 0.1% mM Tween-20, and 1 mg/mL sheared salmon sperm DNA; His, potassium phosphate, 20 mM L-ascorbic acid, 10 μM methylene blue, 1 mM chaps, 10 mM imidazole, and 1 mg/mL sheared salmon sperm DNA (Ambion)] was immobilized on 25 μL of Dynabeads MyOne Streptavidin T1 or IMAC resins (PhyNexus) for 30 min and then washed three times with 200 μL of selection buffer. DEL (5 nmol) in 100 μL of selection buffer was incubated with the immobilized biotin-tagged WDR5 at 25 °C for 1 h and then washed three times with 200 μL of selection buffer to remove unbound DEL molecules. To elute bound molecules, beads were incubated in 100 μL of selection buffer at 95 °C for 10 min. This process was repeated two more times. The same procedure was followed for no target control except without biotin-tagged WDR5.

DNA Sequencing. The general procedure for NGS sequencing sample preparation is outlined as follows: initially, qPCR was conducted to determine the quantity of the DEL selection obtained sample. Subsequently, a PCR experiment was performed using a standard curve established with sample 1, compatible with Illumina sequencing flow cells. The purification of the PCR output product was carried out using Agencourt AMPure XP SPRI beads following the manufacturer's instructions. Following purification, the product quantification was measured using a NanoDrop instrument (Agilent BioAnalyzer) with a high-sensitivity DNA kit. The final concentration of the amplicon for each sample ranged between 3 to 40 nM. Lastly, a portion of the amplified product from each sample was loaded onto the Illumina GAI or HiSeq platform to generate 20 million clusters.

Enrichment Calculation. $\text{Enrichment} = (C/N)/(X/S)$. Enrichment: normalization processing of copy number (C: copy number of the molecule; N: total reads; S: library size; X: real number of the molecule).

Synthesis of Intermediates and Final Compounds. *General Procedure A.* Amide condensation: 3-amino-5-bromobenzoic acid or its analogs (1.5 equiv), amino acids with protected carboxyl groups (1 equiv), *O*-(7-azabenzotriazol-1-yl)-*N,N,N',N'*-tetramethyluronium

hexafluorophosphate (HATU 1.2 equiv), and diisopropylethylamine (3 equiv) were combined in DMF (10 mL) at room temperature. The reaction mixture was stirred for 3 h and then diluted with water. The aqueous layer was extracted with ethyl acetate, and the combined organic layers were washed with brine and dried over anhydrous Na₂SO₄. The resulting mixture was concentrated under vacuum and subjected to purification by flash chromatography, yielding the pure product.

General Procedure B. Reductive amination reaction: 5-methyl-1*H*-imidazole-4-carbaldehyde (1 equiv), aniline analog (1 equiv), sodium triacetoxyborohydride (2 equiv), and trifluoroacetic acid (3 equiv) were introduced into 1,2-dichloroethane (10 mL) at room temperature, and the reaction mixture was stirred overnight. Subsequently, the resulting mixture was concentrated under vacuum and purified through flash chromatography to yield the pure product.

General Procedure C. Suzuki cross-coupling: bromobenzene (1 equiv), boric acid or borate ester (1.2 equiv), dichloro[1,1'-bis(diphenylphosphine)ferrocene]palladium(II) dichloromethane adduct (0.2 equiv), and sodium bicarbonate (2 equiv) were combined in dimethoxyethane:water (3:1). The reaction mixture was stirred at 80 °C for 16 h. Subsequently, the resulting mixture was concentrated under vacuum and purified through flash chromatography to obtain the pure product.

General Procedure D. 5-Bromo-7-nitro-3,4-dihydroisoquinolin-1(2*H*)-one was dissolved in concentrated hydrochloric acid and reacted at 150 °C for 15–20 h. The resulting product was then diluted in water, extracted with ethyl acetate, and subsequently dissolved in water.

General Procedure E. Compounds 31a–b were dissolved in 1,4-dioxane. Then, 2 equiv of titanium tetraisopropoxide was added and reacted at 80 °C for 3 h. Afterward, the reaction was quenched by adding water and the mixture was extracted with ethyl acetate to obtain the product.

(*R*)-3-(4-Chlorophenyl)-2-(4-fluoro-3-((5-methyl-1*H*-imidazole-4-yl)methyl)amino)benzamido)propanoic acid (1). Synthesized according to general procedures A and B to afford 13 mg (30%, solid) of the title compound after HPLC purification. ¹H NMR (400 MHz, MeOD) δ 8.69 (s, 1H), 7.25 (s, 4H), 7.11–7.00 (m, 3H), 4.85–4.78 (m, 1H), 4.44 (s, 2H), 3.36–3.03 (m, 2H), 2.39 (s, 3H). ¹³C NMR (151 MHz, MeOD) δ 174.69, 169.57, 155.80, 154.17,

137.70, 137.37, 133.68, 131.91, 129.44, 127.96, 127.78, 117.66, 115.42, 112.58, 55.53, 37.63, 37.58, 8.96. HRMS(EI) calculated for $C_{21}H_{20}ClFN_4O_3[M]^+$ = 429.1135 found 429.1138.

(*R*)-2-(4-Fluoro-3-(((5-methyl-1*H*-imidazol-4-yl)methyl)amino)benzamido)-3-(4-nitrophenyl)propanoic acid (**2**). Synthesized according to general procedures A and B to afford 14 mg (33%, solid) of the title compound after HPLC purification. 1H NMR (400 MHz, MeOD) δ 8.68 (s, 1H), 8.14 (d, *J* = 8.8 Hz, 2H), 7.51 (d, *J* = 8.7 Hz, 2H), 7.10–7.00 (m, 3H), 4.43 (s, 2H), 3.52–3.18 (m, 2H), 2.38 (s, 3H). ^{13}C NMR (151 MHz, MeOD) δ 174.41, 169.52, 155.82, 154.19, 148.32, 147.12, 137.33, 133.68, 131.84, 131.49, 127.95, 127.77, 124.39, 117.56, 115.44, 112.54, 55.21, 38.14, 37.63, 8.94. HRMS(EI) calculated for $C_{21}H_{20}FN_5O_5[M]^+$ = 440.1376 found 440.1376.

(*R*)-2-(3-Bromo-5-(((5-methyl-1*H*-imidazol-4-yl)methyl)amino)benzamido)-3-(4-chlorophenyl)propanoic acid (**3**). Synthesized according to general procedures A and B to afford 17 mg (40%, solid) of the title compound after HPLC purification. 1H NMR (400 MHz, MeOD) δ 8.68 (s, 1H), 7.25 (t, *J* = 4.0 Hz, 4H), 7.14 (s, 1H), 6.97–6.87 (m, 2H), 4.78 (dd, *J* = 9.6, 5.0 Hz, 1H), 4.36 (s, 2H), 3.37–3.02 (m, 2H), 2.37 (s, 3H). ^{13}C NMR (151 MHz, MeOD) δ 174.81, 168.97, 150.63, 138.00, 137.70, 133.69, 131.91, 129.44, 127.81, 124.01, 119.70, 119.52, 111.06, 55.68, 37.78, 37.56, 8.95. HRMS(EI) calculated for $C_{21}H_{20}BrClN_4O_3[M]^+$ = 489.0335 found 489.0339.

3-Bromo-*N*-(4-chlorophenyl)-5-(((5-methyl-1*H*-imidazol-4-yl)methyl)amino)benzamide (**4**). Synthesized according to general procedures A and B to afford 16 mg (38%, solid) of the title compound after HPLC purification. 1H NMR (400 MHz, MeOD) δ 8.72 (s, 1H), 7.29–7.21 (m, 4H), 7.16 (s, 1H), 6.96 (d, *J* = 10.6 Hz, 2H), 4.38 (s, 2H), 3.54 (t, *J* = 7.3 Hz, 2H), 2.87 (t, *J* = 7.3 Hz, 2H), 2.39 (s, 3H). ^{13}C NMR (151 MHz, MeOD) δ 169.08, 150.69, 139.34, 138.40, 133.70, 133.20, 131.51, 129.51, 127.81, 124.03, 119.51, 119.29, 111.15, 42.34, 37.75, 35.73, 8.92. HRMS(EI) calculated for $C_{20}H_{20}BrClN_4O[M]^+$ = 445.0436 found 445.0437.

(*R*)-3-Bromo-*N*-(3-(4-chlorophenyl)-1-(methylamino)-1-oxopropan-2-yl)-5-(((5-methyl-1*H*-imidazol-4-yl)methyl)amino)benzamide (**5**). **4** was reacted with methylamine hydrochloride (1.2 equiv) following general procedure A to afford 24 mg (80%, solid) of the title compound after HPLC purification. 1H NMR (400 MHz, MeOD) δ 8.71 (s, 1H), 7.28–7.21 (m, 4H), 7.18 (s, 1H), 6.93 (d, *J* = 13.2 Hz, 2H), 4.71 (dd, *J* = 9.0, 6.2 Hz, 1H), 4.37 (s, 2H), 3.21–2.96 (m, 2H), 2.71 (s, 3H), 2.38 (s, 3H). ^{13}C NMR (126 MHz, MeOD) δ 173.78, 168.96, 150.61, 137.87, 137.45, 133.69, 131.90, 129.47, 127.78, 124.01, 119.83, 119.53, 111.18, 56.59, 38.28, 37.72, 26.34, 8.93. HRMS(EI) calculated for $C_{22}H_{23}BrClN_5O_2[M]^+$ = 504.0796 found 504.0798.

(*R*)-3-Bromo-*N*-(3-(4-chlorophenyl)-1-(cyclopropylamino)-1-oxopropan-2-yl)-5-(((5-methyl-1*H*-imidazol-4-yl)methyl)amino)benzamide (**6**). **4** was reacted with cyclopropylamine (1 equiv) following general procedure A to afford 26 mg (83%, solid) of the title compound after HPLC purification. 1H NMR (500 MHz, MeOD) δ 8.71 (s, 1H), 7.25 (q, *J* = 8.6 Hz, 4H), 7.18 (s, 1H), 6.94 (d, *J* = 10.2 Hz, 2H), 4.66 (t, *J* = 7.6 Hz, 1H), 4.37 (s, 2H), 3.15–2.96 (m, 2H), 2.65–2.57 (m, 1H), 2.38 (s, 3H), 0.72–0.62 (m, 2H), 0.46–0.32 (m, 2H). ^{13}C NMR (126 MHz, MeOD) δ 174.70, 168.89, 150.61, 137.86, 137.19, 133.69, 132.01, 129.45, 127.83, 127.78, 124.02, 119.84, 119.52, 111.14, 56.38, 38.41, 37.71, 23.27, 8.94, 6.46, 6.24. HRMS(EI) calculated for $C_{24}H_{25}BrClN_5O_2[M]^+$ = 528.0807 found 528.0806.

(*R*)-*N*-(3-(4-Chlorophenyl)-1-(methylamino)-1-oxopropan-2-yl)-5-(((5-methyl-1*H*-imidazol-4-yl)methyl)amino)-2'-(methylthio)-[1,1'-biphenyl]-3-carboxamide (**7**). Synthesized according to general procedures A–C to afford 18 mg (36%, solid) of the title compound after HPLC purification. 1H NMR (500 MHz, MeOD) δ 8.70 (s, 1H), 7.36–7.31 (m, 2H), 7.26–7.17 (m, 6H), 7.02 (t, *J* = 1.5 Hz, 1H), 7.01–6.99 (m, 1H), 6.79 (dd, *J* = 2.5, 1.4 Hz, 1H), 4.75 (dd, *J* = 8.9, 6.1 Hz, 1H), 4.41 (s, 2H), 3.20–2.97 (m, 2H), 2.71 (s, 3H), 2.36 (s, 3H), 2.34 (s, 3H). ^{13}C NMR (126 MHz, MeOD) δ 173.89, 170.27, 148.91, 143.21, 141.59, 138.28, 137.45, 136.15, 133.62, 133.48, 131.95, 130.79, 129.50, 129.37, 128.38, 127.54, 126.42, 125.80,

118.46, 118.26, 111.82, 56.45, 38.36, 38.15, 26.34, 15.83, 9.01. HRMS(EI) calculated for $C_{29}H_{30}ClN_5O_2S[M]^+$ = 548.1882 found 548.1884.

(*R*)-*N*-(3-(4-chlorophenyl)-1-(methylamino)-1-oxopropan-2-yl)-2'-cyclopropyl-5-(((5-methyl-1*H*-imidazol-4-yl)methyl)amino)-[1,1'-biphenyl]-3-carboxamide (**8**). Synthesized according to general procedures A–C to afford 19 mg (39%, solid) of the title compound after HPLC purification. 1H NMR (500 MHz, MeOD) δ 8.71 (s, 1H), 7.27–7.22 (m, 5H), 7.21–7.11 (m, 2H), 7.08 (t, *J* = 1.5 Hz, 1H), 7.00–6.93 (m, 2H), 6.83 (dd, *J* = 2.4, 1.4 Hz, 1H), 4.76 (dd, *J* = 9.0, 6.0 Hz, 1H), 4.42 (s, 2H), 3.20–2.99 (m, 2H), 2.71 (s, 3H), 2.37 (s, 3H), 1.83–1.66 (m, 1H), 0.79–0.70 (m, 2H), 0.66–0.59 (m, 2H). ^{13}C NMR (126 MHz, MeOD) δ 173.91, 170.42, 149.10, 144.62, 143.22, 141.87, 137.47, 135.99, 133.63, 133.53, 131.92, 130.34, 129.46, 128.85, 128.42, 127.54, 126.30, 125.00, 118.82, 118.74, 110.80, 56.41, 38.35, 38.16, 26.34, 14.25, 10.01, 9.85, 8.97. HRMS(EI) calculated for $C_{31}H_{32}ClN_5O_2[M]^+$ = 542.2317 found 542.2322.

(*R*)-*N*-(3-(4-chlorophenyl)-1-(methylamino)-1-oxopropan-2-yl)-5'-(hydroxymethyl)-2'-methyl-5-(((5-methyl-1*H*-imidazol-4-yl)methyl)amino)-[1,1'-biphenyl]-3-carboxamide (**9**). Synthesized according to general procedures A–C to afford 20 mg (40%, solid) of the title compound after HPLC purification. 1H NMR (500 MHz, MeOD) δ 8.37 (s, 1H), 7.28–7.13 (m, 7H), 7.04 (s, 1H), 6.98 (s, 1H), 6.74 (s, 1H), 4.78 (dd, *J* = 9.4, 5.8 Hz, 1H), 4.59 (s, 2H), 4.36 (s, 2H), 3.24–3.03 (m, 2H), 2.70 (s, 3H), 2.31 (s, 3H), 2.15 (s, 3H). ^{13}C NMR (126 MHz, MeOD) δ 173.96, 170.45, 149.28, 144.39, 142.67, 140.06, 137.50, 135.77, 135.15, 133.75, 133.46, 131.93, 131.33, 129.39, 129.23, 128.97, 127.55, 127.22, 118.19, 110.90, 64.88, 56.65, 38.72, 38.07, 26.40, 20.25, 9.46. HRMS(EI) calculated for $C_{30}H_{32}ClN_5O_3[M]^+$ = 546.2266 found 546.2265.

(*R*)-4'-Chloro-*N*-(3-(4-chlorophenyl)-1-(methylamino)-1-oxopropan-2-yl)-5-(((5-methyl-1*H*-imidazol-4-yl)methyl)amino)-2'-(trifluoromethyl)-[1,1'-biphenyl]-3-carboxamide (**10**). Synthesized according to general procedures A–C to afford 18 mg (32%, solid) of the title compound after HPLC purification. 1H NMR (500 MHz, MeOD) δ 8.71 (s, 1H), 7.78 (s, 1H), 7.68 (d, *J* = 6.0 Hz, 1H), 7.36 (s, 1H), 7.37–7.15 (m, 4H), 7.05 (s, 1H), 6.97 (s, 1H), 6.70 (s, 1H), 4.75 (dd, *J* = 9.0, 6.1 Hz, 1H), 4.41 (s, 2H), 3.19–2.98 (m, 2H), 2.70 (s, 3H), 2.35 (s, 3H). ^{13}C NMR (126 MHz, MeOD) δ 173.84, 169.89, 148.90, 141.10, 137.42, 136.03, 135.02, 134.85, 133.63, 133.54, 132.96, 131.91, 129.46, 128.12, 127.61, 118.03, 117.71, 112.10, 56.48, 38.34, 38.03, 26.33, 8.92. HRMS(EI) calculated for $C_{29}H_{26}Cl_2F_3N_5O_2[M]^+$ = 604.1488 found 604.1489.

(*R*)-*N*-(3-(4-Chlorophenyl)-1-(methylamino)-1-oxopropan-2-yl)-4'-(1,1-difluoroethyl)-5-(((5-methyl-1*H*-imidazol-4-yl)methyl)amino)-[1,1'-biphenyl]-3-carboxamide (**11**). Synthesized according to general procedures A–C to afford 22 mg (42%, solid) of the title compound after HPLC purification. 1H NMR (500 MHz, MeOD) δ 8.71 (s, 1H), 7.69–7.59 (m, 4H), 7.34–7.23 (m, 5H), 7.11–6.93 (m, 2H), 4.77 (dd, *J* = 9.0, 6.1 Hz, 1H), 4.45 (s, 2H), 3.23–3.00 (m, 2H), 2.72 (s, 3H), 2.40 (s, 3H), 2.00–1.90 (m, 3H). ^{13}C NMR (126 MHz, MeOD) δ 173.92, 170.38, 149.88, 143.43, 142.75, 137.51, 136.97, 133.65, 133.60, 131.96, 129.50, 128.30, 128.18, 127.66, 126.25, 116.38, 116.02, 111.55, 56.52, 38.35, 38.05, 26.35, 25.99, 8.97. HRMS(EI) calculated for $C_{30}H_{30}ClF_2N_5O_2[M]^+$ = 566.2129 found 566.2124.

Methyl (*R*)-3-(4-Chlorophenyl)-2-5-(((5-methyl-1*H*-imidazol-4-yl)methyl)amino)-2'-(methylthio)-[1,1'-biphenyl]-3-carboxamido)propanoate (**12**). Synthesized according to general procedures A–C to afford 24 mg (45%, solid) of the title compound after HPLC purification. 1H NMR (600 MHz, MeOD) δ 8.70 (s, 1H), 7.35–7.32 (m, 2H), 7.26–7.21 (m, 6H), 7.00 (s, 2H), 6.79 (s, 1H), 4.86–4.81 (m, 1H), 4.41 (s, 2H), 3.73 (s, 3H), 3.28–3.25 (m, 1H), 3.10–3.04 (m, 1H), 2.36 (s, 3H), 2.34 (s, 3H). ^{13}C NMR (151 MHz, MeOD) δ 173.38, 170.47, 148.90, 143.19, 141.57, 138.29, 137.40, 136.03, 133.67, 133.49, 131.91, 130.78, 129.54, 129.36, 128.37, 127.52, 126.39, 125.79, 118.39, 118.28, 111.83, 55.52, 52.87, 38.13, 37.37, 15.83, 9.01. HRMS(EI) calculated for $C_{29}H_{29}ClN_4O_3S[M]^+$ = 549.1722 found 549.1725.

Methyl (R)-3-(4-Chlorophenyl)-2-(5'-(hydroxymethyl)-2'-methyl-5-(((5-methyl-1H-imidazol-4-yl)methyl)amino)-[1,1'-biphenyl]-3-carboxamido)propanoate (13). Synthesized according to general procedures A–C to afford 28 mg (51%, solid) of the title compound after HPLC purification. ^1H NMR (500 MHz, MeOD) δ 7.77 (s, 1H), 7.29–7.21 (m, 7H), 7.16 (s, 1H), 6.99 (s, 1H), 6.92 (s, 1H), 4.86–4.80 (m, 1H), 4.59 (s, 2H), 4.27 (s, 2H), 3.73 (s, 3H), 3.29–3.25 (m, 1H), 3.13–3.04 (m, 1H), 2.26 (s, 3H), 2.17 (s, 3H). ^{13}C NMR (126 MHz, MeOD) δ 173.45, 170.83, 149.83, 144.45, 142.98, 140.12, 137.46, 135.85, 135.31, 133.70, 131.91, 131.36, 129.54, 129.29, 127.22, 118.20, 117.74, 110.96, 65.00, 55.54, 52.85, 39.94, 37.39, 30.76, 20.22. HRMS(EI) calculated for $\text{C}_{30}\text{H}_{31}\text{ClN}_4\text{O}_4$ $[\text{M}]^+$ = 547.2107 found 547.2106.

2-(4-Chlorophenethyl)-7-(((5-methyl-1H-imidazol-4-yl)methyl)amino)-5-(2-(methylthio)phenyl)-3,4-dihydroisoquinolin-1(2H)-one (14). Synthesized according to general procedures A–E to afford 12 mg (19%, solid) of the title compound after HPLC purification. ^1H NMR (600 MHz, MeOD) δ 8.70 (s, 1H), 7.39–7.33 (m, 1H), 7.30–7.22 (m, 6H), 7.18 (td, J = 7.4, 1.3 Hz, 1H), 7.03 (dd, J = 7.5, 1.5 Hz, 1H), 6.62 (d, J = 2.7 Hz, 1H), 4.40 (s, 2H), 3.78–3.71 (m, 2H), 3.37–3.32 (m, 2H), 2.92 (td, J = 7.1, 2.8 Hz, 2H), 2.49–2.36 (m, 5H), 2.34 (s, 3H). ^{13}C NMR (151 MHz, MeOD) δ 166.90, 147.69, 140.92, 139.68, 139.29, 139.19, 133.44, 133.28, 131.61, 131.18, 130.50, 129.56, 128.49, 127.64, 127.59, 125.58, 119.78, 111.72, 50.52, 48.17, 38.26, 34.16, 25.66, 15.20, 8.99. LC-MS (ESI): m/z = 517.9 $[\text{M} + \text{H}]^+$.

*2-(4-Chlorophenethyl)-8-(((5-methyl-1H-imidazol-4-yl)methyl)amino)-6-(2-(methylthio)phenyl)-2,3,4,5-tetrahydro-1H-benzo[*c*]azepin-1-one (15)*. Synthesized according to general procedures A–C to afford 25 mg (36%, solid) of the title compound after HPLC purification. ^1H NMR (500 MHz, MeOD) δ 8.69 (s, 1H), 7.36 (td, J = 7.6, 1.5 Hz, 1H), 7.29–7.27 (m, 5H), 7.18–7.14 (m, 1H), 7.00 (dd, J = 7.5, 1.5 Hz, 1H), 6.83 (d, J = 2.7 Hz, 1H), 6.51 (d, J = 2.5 Hz, 1H), 4.38 (s, 2H), 3.82–3.77 (m, 2H), 3.25–3.16 (m, 2H), 2.95 (t, J = 7.4 Hz, 2H), 2.39–2.31 (m, 5H), 2.32 (s, 3H), 2.25–2.15 (m, 2H). ^{13}C NMR (126 MHz, MeOD) δ 173.79, 147.26, 141.59, 140.45, 139.55, 139.10, 138.43, 133.41, 133.28, 131.60, 130.43, 129.54, 129.40, 128.47, 127.55, 126.04, 125.40, 125.27, 118.28, 112.98, 50.08, 48.31, 38.16, 34.97, 30.69, 26.15, 15.16, 8.99. LC-MS (ESI): m/z = 531.9 $[\text{M} + \text{H}]^+$.

2-(4-Chlorophenethyl)-5-(5-(hydroxymethyl)-2-methylphenyl)-7-(((5-methyl-1H-imidazol-4-yl)methyl)amino)-3,4-dihydroisoquinolin-1(2H)-one (16). Synthesized according to general procedures A–E to afford 10 mg (12%, solid) of the title compound after HPLC purification. ^1H NMR (400 MHz, MeOD) δ 8.70 (s, 1H), 7.25 (d, J = 2.7 Hz, 6H), 7.21 (d, J = 2.6 Hz, 1H), 7.03 (s, 1H), 6.63 (d, J = 2.6 Hz, 1H), 4.58 (s, 2H), 4.41 (s, 2H), 3.75 (t, J = 7.3 Hz, 2H), 3.34 (d, J = 6.8 Hz, 2H), 2.93 (dd, J = 7.9, 6.5 Hz, 2H), 2.39 (s, 3H), 2.39–2.26 (m, 2H), 2.00 (s, 3H). ^{13}C NMR (151 MHz, MeOD) δ 166.94, 147.77, 142.42, 141.11, 140.26, 139.19, 135.81, 133.46, 133.29, 131.61, 131.23, 131.06, 129.55, 128.92, 128.51, 127.59, 127.56, 127.12, 119.42, 111.04, 64.86, 50.50, 48.16, 38.24, 34.16, 25.70, 19.57, 8.98. LC-MS (ESI): m/z = 515.9 $[\text{M} + \text{H}]^+$.

5-(4-Chloro-2-(trifluoromethyl)phenyl)-2-(4-chlorophenethyl)-7-(((5-methyl-1H-imidazol-4-yl)methyl)amino)-3,4-dihydroisoquinolin-1(2H)-one (17). Synthesized according to general procedures A–E to afford 12 mg (14%, solid) of the title compound after HPLC purification. ^1H NMR (500 MHz, MeOD) δ 8.71 (s, 1H), 7.81 (s, 1H), 7.68 (d, J = 8.4 Hz, 1H), 7.29–7.22 (m, 6H), 6.62 (s, 1H), 4.40 (s, 2H), 3.81–3.68 (m, 2H), 3.41–3.33 (m, 2H), 2.92 (t, J = 7.3 Hz, 2H), 2.43–2.21 (m, 5H). ^{13}C NMR (126 MHz, MeOD) δ 145.84, 137.74, 137.01, 133.86, 133.28, 132.11, 131.92, 131.79, 130.18, 129.75, 128.16, 126.92, 125.82, 117.88, 110.78, 49.11, 46.48, 36.76, 32.73, 24.54, 7.52. LC-MS (ESI): m/z = 573.8 $[\text{M} + \text{H}]^+$.

2-(4-Chlorophenethyl)-5-(4-fluoro-2-(methylthio)phenyl)-7-(((5-methyl-1H-imidazol-4-yl)methyl)amino)-3,4-dihydroisoquinolin-1(2H)-one (18). Synthesized according to general procedures A–E to afford 19 mg (23%, solid) of the title compound after HPLC purification. ^1H NMR (600 MHz, MeOD) δ 8.70 (s, 1H), 7.28–7.21 (m, 5H), 7.06–7.01 (m, 2H), 6.93–6.87 (m, 1H), 6.61 (d, J = 2.6 Hz, 1H), 4.40 (s, 2H), 3.80–3.70 (m, 2H), 3.35–3.32 (m, 2H), 2.95–

2.88 (m, 2H), 2.45–2.33 (m, 8H). ^{13}C NMR (151 MHz, MeOD) δ 166.80, 165.14, 163.51, 147.75, 142.47, 139.81, 139.18, 135.29, 133.78, 133.46, 133.28, 133.05, 132.00, 131.60, 131.30, 130.02, 129.56, 128.42, 127.83, 127.62, 119.96, 111.93, 50.51, 48.14, 38.25, 34.15, 25.59, 15.04, 8.99. LC-MS (ESI): m/z = 535.9 $[\text{M} + \text{H}]^+$.

2-(4-Chlorobenzyl)-7-(((5-methyl-1H-imidazol-4-yl)methyl)amino)-5-(2-(methylthio)phenyl)-3,4-dihydroisoquinolin-1(2H)-one (19). Synthesized according to general procedures A–E to afford 13 mg (21%, solid) of the title compound after HPLC purification. ^1H NMR (600 MHz, MeOD) δ 8.71 (s, 1H), 7.37–7.29 (m, 7H), 7.18 (td, J = 7.4, 1.2 Hz, 1H), 7.05 (dd, J = 7.5, 1.4 Hz, 1H), 6.65 (d, J = 2.6 Hz, 1H), 4.73 (s, 2H), 4.42 (s, 2H), 3.43–3.37 (m, 2H), 2.56–2.46 (m, 2H), 2.39 (s, 3H), 2.34 (s, 3H). ^{13}C NMR (151 MHz, MeOD) δ 167.14, 147.78, 141.04, 139.62, 139.28, 137.47, 134.36, 133.46, 131.00, 130.53, 130.47, 129.80, 129.58, 128.48, 127.61, 125.57, 120.01, 111.95, 51.00, 47.21, 38.26, 25.73, 15.15, 8.99. LC-MS (ESI): m/z = 503.9 $[\text{M} + \text{H}]^+$.

2-(4-Chlorobenzyl)-5-(5-(hydroxymethyl)-2-methylphenyl)-7-(((5-methyl-1H-imidazol-4-yl)methyl)amino)-3,4-dihydroisoquinolin-1(2H)-one (20). Synthesized according to general procedures A–E to afford 14 mg (16%, solid) of the title compound after HPLC purification. ^1H NMR (500 MHz, MeOD) δ 8.05 (s, 1H), 7.35–7.29 (m, 5H), 7.23 (s, 2H), 7.03 (s, 1H), 6.65 (s, 1H), 4.77–4.68 (m, 2H), 4.56 (s, 2H), 4.31 (s, 2H), 3.38 (t, J = 6.6 Hz, 2H), 2.53–2.38 (m, 2H), 2.31 (s, 3H), 2.01 (s, 3H). ^{13}C NMR (126 MHz, MeOD) δ 167.30, 148.29, 142.31, 141.24, 140.18, 137.51, 135.85, 134.30, 134.10, 131.04, 130.92, 130.49, 129.78, 129.00, 127.46, 126.50, 119.43, 111.66, 64.87, 50.95, 39.42, 25.80, 19.65, 9.70. LC-MS (ESI): m/z = 501.9 $[\text{M} + \text{H}]^+$.

2-(4-Chlorobenzyl)-5-(4-fluoro-2-(methylthio)phenyl)-7-(((5-methyl-1H-imidazol-4-yl)methyl)amino)-3,4-dihydroisoquinolin-1(2H)-one (21). Synthesized according to general procedures A–E to afford 16 mg (19%, solid) of the title compound after HPLC purification. ^1H NMR (600 MHz, MeOD) δ 8.71 (s, 1H), 7.32 (d, J = 14.0 Hz, 5H), 7.07–7.02 (m, 2H), 6.92–6.88 (m, 1H), 6.64 (d, J = 2.6 Hz, 1H), 4.73 (s, 2H), 4.42 (s, 2H), 3.42–3.37 (m, 2H), 2.54–2.48 (m, 2H), 2.39 (s, 3H), 2.36 (s, 3H). ^{13}C NMR (151 MHz, MeOD) δ 167.05, 165.15, 163.52, 147.87, 142.47, 139.92, 137.46, 135.24, 134.37, 133.48, 132.09, 131.12, 130.49, 129.81, 128.42, 127.75, 127.65, 120.17, 112.15, 111.91, 111.80, 50.99, 47.17, 38.22, 25.66, 14.99, 8.99. LC-MS (ESI): m/z = 521.9 $[\text{M} + \text{H}]^+$.

Docking Study. The docking study was conducted using AutoDock Vina. The WDR5 protein structure was obtained from the Protein Data Bank (PDB: 6E22). Both the protein and compound 11a structures underwent preprocessing with AutoDock Tools prior to docking. The center coordinates of the grid box were determined based on the cocrystallized ligand structure. Subsequently, semi-flexible docking was performed with default parameter settings. The selection of the binding mode was based on docking scores and energy. The results of the docking were visualized and analyzed using PyMOL.

WDR5 HTRF Assay. The compounds for testing were diluted 3-fold with DMSO, establishing 12 concentration gradients with 2 replicates for each concentration. The reaction buffer consisted of 25 mM HEPES at pH 7.5, 100 mM NaCl, and 0.05% Tween 20. In 384-well plates, 120 nL of the compound and 4 μL of 37.5 nM WDR5 protein were added, centrifuged at 1000 rpm for 1 min, and incubated at room temperature for 30 min, and then 4 μL of 300 nM MLL1 peptide was introduced. Following a 10 min incubation at room temperature, 4 μL of Anti-6His-Eu cryptate and streptavidin-APC mixture were added, centrifuged at 1000 rpm for 1 min, and incubated at room temperature for 60 min in the dark. Signal readings were obtained using a multilabel microplate reader (EnVision 2105). Each plate included the following controls: a control group (120 nL DMSO, 4 μL 37.5 nM WDR5, 4 μL MLL1 peptide, 4 μL Anti-6His-Eu cryptate, and streptavidin-APC) and a blank group (120 nL DMSO, 4 μL reaction buffer, 4 μL MLL1 peptide, 4 μL Anti-6His-Eu cryptate, and streptavidin-APC). Test data were calculated based on the signal ratio of two fluorescent beams with different wavelengths: (signal at 665 nm/signal at 620 nm) \times 10000. The inhibition rate was

determined by the formula: inhibition rate (%) = 100 - (experimental group - blank group)/(control group - blank group) × 100. IC₅₀ values were calculated using XLfit software.

Cell Growth Inhibition Assay. The MV4-11 and K562 cell lines were procured from the National Collection of Authenticated Cell Cultures in Shanghai, China, and underwent authentication through subsequent STR analysis. Both cell lines were cultured in IMDM (Gibco, C12440500BT) supplemented with 10% fetal bovine serum (Gibco, 10091-148). For the experiments, testing compounds were serially diluted in 96-well plates. Subsequently, cells were seeded into the wells at a density of 1,000 and 1,000 cells/well for MV4-11 and K562, respectively. The plated cells were then incubated with 5% CO₂ at 37 °C for 5 days. Following this incubation period, the cell viability was measured using the cell counting kit-8 reagent (Dojindo) in accordance with the manufacturer's protocols. The absorbance at OD450 was detected using a multimode microplate reader (TECAN SPARK 10 M). The untreated cells were considered as 100% cell viability. The IC₅₀ values were calculated by fitting a nonlinear regression curve in GraphPad Prism.

■ ASSOCIATED CONTENT

SI Supporting Information

The Supporting Information is available free of charge at <https://pubs.acs.org/doi/10.1021/acs.jmedchem.3c01463>.

Experimental procedure for DNA-encoded library synthesis; biochemical assay; small molecules with H NMR, ¹³C NMR, and HPLC spectra (PDF)

Molecular formula string (CSV) (CSV)

■ AUTHOR INFORMATION

Corresponding Authors

Yujun Zhao – State Key Laboratory of Drug Research, Shanghai Institute of Materia Medica, Chinese Academy of Sciences, Shanghai 201203, China; University of Chinese Academy of Sciences, Beijing 100049, China; orcid.org/0000-0003-1035-2272; Email: yjzhao@simm.ac.cn

Zhiqiang Duan – State Key Laboratory of Drug Research, Shanghai Institute of Materia Medica, Chinese Academy of Sciences, Shanghai 201203, China; Email: duanzq@simm.ac.cn

Jidong Zhu – Etern BioPharma (Shanghai) Co., Ltd., Shanghai 201203, China; Email: zhujidong@eternbio.com

Xiaojie Lu – School of Chinese Materia Medica, Nanjing University of Chinese Medicine, Nanjing 210023, China; State Key Laboratory of Drug Research, Shanghai Institute of Materia Medica, Chinese Academy of Sciences, Shanghai 201203, China; University of Chinese Academy of Sciences, Beijing 100049, China; orcid.org/0000-0002-3600-288X; Email: xjlu@simm.ac.cn

Authors

Shaozhao Qin – School of Chinese Materia Medica, Nanjing University of Chinese Medicine, Nanjing 210023, China; State Key Laboratory of Drug Research, Shanghai Institute of Materia Medica, Chinese Academy of Sciences, Shanghai 201203, China

Lijian Feng – Etern BioPharma (Shanghai) Co., Ltd., Shanghai 201203, China

Qingyi Zhao – School of Chinese Materia Medica, Nanjing University of Chinese Medicine, Nanjing 210023, China; State Key Laboratory of Drug Research, Shanghai Institute of Materia Medica, Chinese Academy of Sciences, Shanghai 201203, China

Ziqin Yan – State Key Laboratory of Drug Research, Shanghai Institute of Materia Medica, Chinese Academy of Sciences, Shanghai 201203, China

Xilin Lyu – State Key Laboratory of Drug Research, Shanghai Institute of Materia Medica, Chinese Academy of Sciences, Shanghai 201203, China

Kaige Li – School of Chinese Materia Medica, Nanjing University of Chinese Medicine, Nanjing 210023, China; State Key Laboratory of Drug Research, Shanghai Institute of Materia Medica, Chinese Academy of Sciences, Shanghai 201203, China

Baiyang Mu – State Key Laboratory of Drug Research, Shanghai Institute of Materia Medica, Chinese Academy of Sciences, Shanghai 201203, China

Yujie Chen – State Key Laboratory of Drug Research, Shanghai Institute of Materia Medica, Chinese Academy of Sciences, Shanghai 201203, China; University of Chinese Academy of Sciences, Beijing 100049, China

Weiwei Lu – State Key Laboratory of Drug Research, Shanghai Institute of Materia Medica, Chinese Academy of Sciences, Shanghai 201203, China

Chao Wang – State Key Laboratory of Drug Research, Shanghai Institute of Materia Medica, Chinese Academy of Sciences, Shanghai 201203, China; University of Chinese Academy of Sciences, Beijing 100049, China

Yanrui Suo – State Key Laboratory of Drug Research, Shanghai Institute of Materia Medica, Chinese Academy of Sciences, Shanghai 201203, China; University of Chinese Academy of Sciences, Beijing 100049, China

Jinfeng Yue – State Key Laboratory of Drug Research, Shanghai Institute of Materia Medica, Chinese Academy of Sciences, Shanghai 201203, China

Mengqing Cui – State Key Laboratory of Drug Research, Shanghai Institute of Materia Medica, Chinese Academy of Sciences, Shanghai 201203, China

Yingjie Li – Etern BioPharma (Shanghai) Co., Ltd., Shanghai 201203, China

Complete contact information is available at:

<https://pubs.acs.org/doi/10.1021/acs.jmedchem.3c01463>

Author Contributions

*S.Z.Q. and L.J.F. contributed equally to this article. S.Z.Q., L.J.F., Z.Q.D., Y.J.Z., J.D.Z., and X.J.L. planned and designed experiments. S.Z.Q., Q.Y.Z., K.G.L., and B.Y.M. carried out the work including DEL construction and syntheses off-DNA small molecules. J.F.Y., W.W.L., and M.Q.C. performed the affinity DEL selection. Z.Q.D., Y.J.C., and Y.R.S. executed the analysis of the screening data. C.W. performed molecular docking study; L.J.F. and Y.J.L. carried out the HTRF assay; Z.Q.Y. and X.L.L. executed the cell growth inhibition assay. Y.J.Z., Z.Q.D., J.D.Z., and X.J.L. prepared the manuscript.

Notes

The authors declare no competing financial interest.

■ ACKNOWLEDGMENTS

This work was supported by the National Natural Science Foundation of China (NSFC 91953203, 92253305, 21907105, and 82073682), Shanghai Pujiang Program (no. 2019PJD056), Science and Technology Commission of Shanghai Municipality (no. 21ZR1475000 and 22ZR1475000), and Shanghai Municipal Science and Technology Major Project for financial support of this work.

■ ABBREVIATIONS

AOP, Fmoc-15-amino-4,7,10,13-tetraoxapentadecanoic acid; BB, building block; DEL, DNA-encoded library; DMSO, dimethyl sulfoxide; HATU, 1*H*-1,2,3-triazolo[4,5-*b*]pyridinium; HP, headpiece; HPLC, high-performance liquid chromatography; HTRF, homogeneous time-resolved fluorescence; IC₅₀, half-maximum inhibitory; MLL1, mixed-lineage leukemia 1; MLL-r, MLL rearrangement; MS, mass spectrometry; NAD⁺, nicotinamide adenine dinucleotide; NTC, no target control; PDB, Protein Data Bank; PROTACs, proteolysis-targeting chimeras; rt, room temperature; SAR, structure–activity relationship; TLC, thin-layer chromatography; TOF, time of flight; WBM, WDR5 binding motif; WDR5, WD repeat domain 5; WIN, WDR5 interaction motif

■ REFERENCES

- (1) Guarnaccia, A. D.; Tansey, W. P. Moonlighting with WDR5: A Cellular Multitasker. *J. Clin. Med.* **2018**, *7*, 21.
- (2) Chen, X.; Xu, J.; Wang, X.; Long, G.; You, Q.; Guo, X. Targeting WD Repeat-Containing Protein 5 (WDR5): A Medicinal Chemistry Perspective. *J. Med. Chem.* **2021**, *64*, 10537–10556.
- (3) Guarnaccia, A. D.; Rose, K. L.; Wang, J.; Zhao, B.; Popay, T. M.; Wang, C. E.; Guerrazzi, K.; Hill, S.; Woodley, C. M.; Hansen, T. J.; Lorey, S. L.; Shaw, J. G.; Payne, W. G.; Weissmiller, A. M.; Olejniczak, E. T.; Fesik, S. W.; Liu, Q.; Tansey, W. P. Impact of WIN site inhibitor on the WDR5 interactome. *Cell Rep.* **2021**, *34*, No. 108636.
- (4) Ruthenburg, A. J.; Wang, W.; Graybosch, D. M.; Li, H.; Allis, C. D.; Patel, D. J.; Verdine, G. L. Histone H3 recognition and presentation by the WDR5 module of the MLL1 complex. *Nat. Struct. Mol. Biol.* **2006**, *13*, 704–712.
- (5) Liu, L.; Guo, X.; Wang, Y.; Li, G.; Yu, Y.; Song, Y.; Zeng, C.; Ding, Z.; Qiu, Y.; Yan, F.; Zhang, Y. X.; Zhao, C.; Zhang, Y.; Dou, Y.; Atadja, P.; Li, E.; Wang, H. Loss of Wdr5 attenuates MLL-rearranged leukemogenesis by suppressing Myc targets. *Biochim. Biophys. Acta Mol. Basis Dis.* **2023**, *1869*, No. 166600.
- (6) Ye, X.; Chen, G.; Jin, J.; Zhang, B.; Wang, Y.; Cai, Z.; Ye, F. The Development of Inhibitors Targeting the Mixed Lineage Leukemia 1 (MLL1)-WD Repeat Domain 5 Protein (WDR5) Protein-Protein Interaction. *Curr. Med. Chem.* **2020**, *27*, 5530–5542.
- (7) Karatas, H.; Li, Y.; Liu, L.; Ji, J.; Lee, S.; Chen, Y.; Yang, J.; Huang, L.; Bernard, D.; Xu, J.; Townsend, E. C.; Cao, F.; Ran, X.; Li, X.; Wen, B.; Sun, D.; Stuckey, J. A.; Lei, M.; Dou, Y.; Wang, S. Discovery of a Highly Potent, Cell-Permeable Macrocyclic Peptidomimetic (MM-589) Targeting the WD Repeat Domain 5 Protein (WDR5)-Mixed Lineage Leukemia (MLL) Protein-Protein Interaction. *J. Med. Chem.* **2017**, *60*, 4818–4839.
- (8) Senisterra, G.; Wu, H.; Allali-Hassani, A.; Wasney, G. A.; Barsyte-Lovejoy, D.; Dombrowski, L.; Dong, A.; Nguyen, K. T.; Smil, D.; Bolshan, Y.; Hajian, T.; He, H.; Seitova, A.; Chau, I.; Li, F.; Poda, G.; Couture, J. F.; Brown, P. J.; Al-Awar, R.; Schapira, M.; Arrowsmith, C. H.; Vedadi, M. Small-molecule inhibition of MLL activity by disruption of its interaction with WDR5. *Biochem. J.* **2013**, *449*, 151–159.
- (9) Chen, W.; Chen, X.; Li, D.; Zhou, J.; Jiang, Z.; You, Q.; Guo, X. Discovery of DDO-2213 as a Potent and Orally Bioavailable Inhibitor of the WDR5-Mixed Lineage Leukemia 1 Protein-Protein Interaction for the Treatment of MLL Fusion Leukemia. *J. Med. Chem.* **2021**, *64*, 8221–8245.
- (10) Wang, F.; Jeon, K. O.; Salovich, J. M.; Macdonald, J. D.; Alvarado, J.; Gogliotti, R. D.; Phan, J.; Olejniczak, E. T.; Sun, Q.; Wang, S.; Camper, D.; Yuh, J. P.; Shaw, J. G.; Sai, J.; Rossanese, O. W.; Tansey, W. P.; Stauffer, S. R.; Fesik, S. W. Discovery of Potent 2-Aryl-6,7-dihydro-5*H*-pyrrolo[1,2-*a*]imidazoles as WDR5-WIN-Site Inhibitors Using Fragment-Based Methods and Structure-Based Design. *J. Med. Chem.* **2018**, *61*, 5623–5642.
- (11) Tian, J.; Teuscher, K. B.; Aho, E. R.; Alvarado, J. R.; Mills, J. J.; Meyers, K. M.; Gogliotti, R. D.; Han, C.; Macdonald, J. D.; Sai, J.; Shaw, J. G.; Sensintaffar, J. L.; Zhao, B.; Rietz, T. A.; Thomas, L. R.; Payne, W. G.; Moore, W. J.; Stott, G. M.; Kondo, J.; Inoue, M.; Coffey, R. J.; Tansey, W. P.; Stauffer, S. R.; Lee, T.; Fesik, S. W. Discovery and Structure-Based Optimization of Potent and Selective WD Repeat Domain 5 (WDR5) Inhibitors Containing a Dihydroisoquinolinone Bicyclic Core. *J. Med. Chem.* **2020**, *63*, 656–675.
- (12) Teuscher, K. B.; Meyers, K. M.; Wei, Q.; Mills, J. J.; Tian, J.; Alvarado, J.; Sai, J.; Van Meveren, M.; South, T. M.; Rietz, T. A.; Zhao, B.; Moore, W. J.; Stott, G. M.; Tansey, W. P.; Lee, T.; Fesik, S. W. Discovery of Potent Orally Bioavailable WD Repeat Domain 5 (WDR5) Inhibitors Using a Pharmacophore-Based Optimization. *J. Med. Chem.* **2022**, *65*, 6287–6312.
- (13) Dolle, A.; Adhikari, B.; Kramer, A.; Weckesser, J.; Berner, N.; Berger, L. M.; Diebold, M.; Szweczyk, M. M.; Barysht-Lovejoy, D.; Arrowsmith, C. H.; Gebel, J.; Lohr, F.; Dotsch, V.; Eilers, M.; Heinzlmeier, S.; Kuster, B.; Sotriffer, C.; Wolf, E.; Knapp, S. Design, Synthesis, and Evaluation of WD-Repeat-Containing Protein 5 (WDR5) Degraders. *J. Med. Chem.* **2021**, *64*, 10682–10710.
- (14) Zimmermann, G.; Neri, D. DNA-encoded chemical libraries: foundations and applications in lead discovery. *Drug Discovery Today* **2016**, *21*, 1828–1834.
- (15) Song, M.; Hwang, G. T. DNA-Encoded Library Screening as Core Platform Technology in Drug Discovery: Its Synthetic Method Development and Applications in DEL Synthesis. *J. Med. Chem.* **2020**, *63*, 6578–6599.
- (16) Kleiner, R. E.; Dumelin, C. E.; Liu, D. R. Small-molecule discovery from DNA-encoded chemical libraries. *Chem. Soc. Rev.* **2011**, *40*, 5707–5717.
- (17) Brenner, S.; Lerner, R. A. Encoded combinatorial chemistry. *Proc. Natl. Acad. Sci. U.S.A.* **1992**, *89*, 5381–5383.
- (18) Arico-Muendel, C. C. From haystack to needle: finding value with DNA encoded library technology at GSK. *MedChemComm* **2016**, *7*, 1898–1909.
- (19) Yuen, L. H.; Franzini, R. M. Achievements, Challenges, and Opportunities in DNA-Encoded Library Research: An Academic Point of View. *Chembiochem* **2017**, *18*, 829–836.
- (20) Zhu, H.; Flanagan, M. E.; Stanton, R. V. Designing DNA Encoded Libraries of Diverse Products in a Focused Property Space. *J. Chem. Inf. Model.* **2019**, *59*, 4645–4653.
- (21) Salvini, C. L. A.; Darlot, B.; Davison, J.; Martin, M. P.; Tudhope, S. J.; Turberville, S.; Kawamura, A.; Noble, M. E. M.; Wedge, S. R.; Crawford, J. J.; Waring, M. J. Fragment expansion with NUDELs - poised DNA-encoded libraries. *Chem. Sci.* **2023**, *14*, 8288–8294.
- (22) Yuen, L. H.; Dana, S.; Liu, Y.; Bloom, S. I.; Thorsell, A. G.; Neri, D.; Donato, A. J.; Kireev, D.; Schuler, H.; Franzini, R. M. A Focused DNA-Encoded Chemical Library for the Discovery of Inhibitors of NAD⁺-Dependent Enzymes. *J. Am. Chem. Soc.* **2019**, *141*, 5169–5181.
- (23) Dawadi, S.; Simmons, N.; Miklosy, G.; Bohren, K. M.; Faver, J. C.; Ucisik, M. N.; Nyshadham, P.; Yu, Z.; Matzuk, M. M. Discovery of potent thrombin inhibitors from a protease-focused DNA-encoded chemical library. *Proc. Natl. Acad. Sci. U.S.A.* **2020**, *117*, 16782–16789.
- (24) Gibaut, Q. M. R.; Akahori, Y.; Bush, J. A.; Taghavi, A.; Tanaka, T.; Aikawa, H.; Ryan, L. S.; Paegel, B. M.; Disney, M. D. Study of an RNA-Focused DNA-Encoded Library Informs Design of a Degrader of a r(CUG) Repeat Expansion. *J. Am. Chem. Soc.* **2022**, *144*, 21972–21979.
- (25) Zambaldo, C.; Daguier, J. P.; Saarbach, J.; Barluenga, S.; Winssinger, N. Screening for covalent inhibitors using DNA-display of small molecule libraries functionalized with cysteine reactive moieties. *MedChemComm* **2016**, *7*, 1340–1351.
- (26) Stress, C. J.; Sauter, B.; Schneider, L. A.; Sharpe, T.; Gillingham, D. A DNA-Encoded Chemical Library Incorporating Elements of Natural Macrocycles. *Angew. Chem., Int. Ed. Engl.* **2019**, *58*, 9570–9574.
- (27) Ma, P.; Xu, H.; Li, J.; Lu, F.; Ma, F.; Wang, S.; Xiong, H.; Wang, W.; Buratto, D.; Zonta, F.; Wang, N.; Liu, K.; Hua, T.; Liu, Z.

J.; Yang, G.; Lerner, R. A. Functionality-Independent DNA Encoding of Complex Natural Products. *Angew. Chem., Int. Ed. Engl.* **2019**, *58*, 9254–9261.

(28) Rianjongdee, F.; Atkinson, S. J.; Chung, C. W.; Grandi, P.; Gray, J. R. J.; Kaushansky, L. J.; Medeiros, P.; Messenger, C.; Phillipou, A.; Preston, A.; Prinjha, R. K.; Rioja, I.; Satz, A. L.; Taylor, S.; Wall, I. D.; Watson, R. J.; Yao, G.; Demont, E. H. Discovery of a Highly Selective BET BD2 Inhibitor from a DNA-Encoded Library Technology Screening Hit. *J. Med. Chem.* **2021**, *64*, 10806–10833.

(29) Montoya, A. L.; Glavatskikh, M.; Halverson, B. J.; Yuen, L. H.; Schuler, H.; Kireev, D.; Franzini, R. M. Combining pharmacophore models derived from DNA-encoded chemical libraries with structure-based exploration to predict Tankyrase 1 inhibitors. *Eur. J. Med. Chem.* **2023**, *246*, No. 114980.

(30) Peterson, A. A.; Liu, D. R. Small-molecule discovery through DNA-encoded libraries. *Nat. Rev. Drug. Discovery* **2023**, *22*, 699–722.

(31) Franzini, R. M.; Ekblad, T.; Zhong, N.; Wichert, M.; Decurtins, W.; Nauer, A.; Zimmermann, M.; Samain, F.; Scheuermann, J.; Brown, P. J.; Hall, J.; Gräslund, S.; Schüler, H.; Neri, D. Identification of Structure-Activity Relationships from Screening a Structurally Compact DNA-Encoded Chemical Library. *Angew. Chem., Int. Ed.* **2015**, *54*, 3927–3931.

(32) Denton, K. E.; Wang, S.; Gignac, M. C.; Milosevich, N.; Hof, F.; Dykhuizen, E. C.; Krusemark, C. J. Robustness of In Vitro Selection Assays of DNA-Encoded Peptidomimetic Ligands to CBX7 and CBX8. *SLAS Discovery* **2018**, *23*, 417–428.

(33) Wang, S.; Alpsoy, A.; Sood, S.; Ordonez-Rubiano, S. C.; Dhiman, A.; Sun, Y.; Jiao, G.; Krusemark, C. J.; Dykhuizen, E. C. A Potent, Selective CBX2 Chromodomain Ligand and Its Cellular Activity During Prostate Cancer Neuroendocrine Differentiation. *Chembiochem* **2021**, *22*, 2335–2344.

(34) Wang, S.; Denton, K. E.; Hobbs, K. F.; Weaver, T.; McFarlane, J. M. B.; Connelly, K. E.; Gignac, M. C.; Milosevich, N.; Hof, F.; Paci, I.; Musselman, C. A.; Dykhuizen, E. C.; Krusemark, C. J. Optimization of Ligands Using Focused DNA-Encoded Libraries To Develop a Selective, Cell-Permeable CBX8 Chromodomain Inhibitor. *ACS Chem. Biol.* **2020**, *15*, 112–131.